AGRICULTURE AND NATURAL RESOURCES

Journal homepage: http://anres.kasetsart.org

Research article

Determining suitable meteorological drought and vegetation indices for monitoring drought and crop yield in Srepok River basin, Vietnam

Huynh Cong Luc*, Luong Van Viet, Bui Dang Hung

Institute of Environmental Science, Engineering and Management, Industrial University of Ho Chi Minh City, Ho Chi Minh City 700000, Vietnam

Article Info

Article history:
Received 10 September 2024
Revised 30 December 2024
Accepted 10 February 2025
Available online 28 February 2025

Keywords:
Crop yield,
Meteorological drought,
Srepok River basin,
Standardized precipitation index,
Vegetation index

Abstract

Importance of the work: Drought is a severe natural disaster that damages crop yields.
Objectives: To identify suitable meteorological drought and vegetation indices for monitoring drought and crop yield in the Srepok basin, Vietnam.
Materials and Methods: The study used the standardized precipitation index (SPI), effective drought index (EDI), vegetation health index (VHI), vegetation condition index (VCI), temperature condition index (TCI) and crop yields from 2000 to 2022. Simple and multiple correlation coefficients between these indices and crop yields were analyzed.
Results: SPI had a better relationship with the vegetation indices and crop yields than EDI. VHI, TCI and VCI, in descending order, had good relationships with meteorological drought indices. The pairing of VHI and the SPI at a 6-month time scale (SPI6) was the most suitable for monitoring drought in the study area during the dry season (February to early May). The best choice for crop yields was the SPI at a 5-month time scale (SPI5), taken at 9 mth and 3 mth before harvest for warning of the impact of drought on coffee and winter-spring rice, respectively.
Main finding: In the Srepok River basin, the SPI6-VHI combination was most effective for drought monitoring during February–May, while SPI5 with different lead times (9 mth for coffee and 3 mth for rice) provided optimal yield forecasting.

* Corresponding author.
E-mail address: huynhcongluc@iuh.edu.vn (H.C. Luc)

https://doi.org/10.34044/j.anres.2025.59.2.09

Introduction

Drought, a natural phenomenon that is difficult to predict, is becoming more severe due to the effects of climate change and human activity (Mishra and Singh, 2010; Mukherjee et al., 2018). Studies have shown that drought has a serious impact on many aspects of social life and the environment on a global scale, with the level of impact varying by region (Leng et al., 2015; Hamal et al., 2020). In particular, drought reduces soil moisture and affects plant growth, reducing yields and food security (Haile et al., 2020). Short-term drought can affect plant growth and reproduction, while long-term drought can cause larger changes in the structure and function of ecosystems (Manatsa et al., 2010). Often, regions with a primarily nature-based agricultural sector are severely affected by drought (Miyan, 2015). Therefore, early detection and monitoring of drought are essential to minimize economic and environmental damage and ensure food security (Khoi et al., 2021).

The severity of drought has been quantified using many drought indices based on climate variables such as precipitation, temperature, and soil moisture (Mishra and Singh, 2010; Zargar et al., 2011). Of these, several that have been widely used are: the Palmer drought severity index (Palmer, 1965), the standardized precipitation index (SPI; McKee et al., 1993), the effective drought index (EDI; Byun and Wilhite, 1999) and the standardized precipitation evapotranspiration index (Vicente-Serrano et al., 2010). Huang et al. 9(2016) and Bhunia et al. (2019) used the SPI to assess the severity and frequency of droughts and indicated an increase in dry events. The SPI allowed for adjusting the time scale, from short-term to long-term, which helped to accurately reflect the impacts of drought on vegetation and crop yields (Prajapati et al., 2021; Vélez-Nicolás et al., 2022). In addition, the EDI was considered a useful tool for quantifying short-term drought events in Australia (Deo et al., 2016). The strength of the EDI was in its ability to accurately analyze and detect the spatial and temporal characteristics of drought; therefore, it was an effective tool for capturing the changes in vegetation and crop yields due to drought (Anshuka et al., 2021). Studies in India (Jain et al., 2015) and South Korea (Kim et al., 2009) indicated that the SPI and EDI provided more accurate and consistent results than other drought indices, highlighting their importance in drought monitoring and assessment.

Although meteorological drought indices are often effective when applied to individual meteorological stations, they are not very effective at the regional level (Son et al., 2012), mainly due to the limited number of observation stations, which means that the scope of the meteorological data collected is not sufficient to support the timely identification, monitoring, and decision-making regarding drought (AghaKouchak et al., 2015). In large regions, the use of satellite data may be a useful alternative, as they allow for drought monitoring on a wide scale, especially in areas with sparse population density and harsh environmental conditions (Himanshu et al., 2015). Drought monitoring based on satellite-derived products is considered to be useful and important (Tran et al., 2017). In addition, agricultural monitoring systems have included indices derived from the spectral reflectance of vegetation to provide accurate and timely information about seasonal plant growth (Thao et al., 2022). Many techniques have been developed to describe agricultural drought based on satellite data at regional and global scales, such as the normalized difference vegetation index (NDVI) (Holben et al., 1980), the vegetation condition index (VCI), the temperature condition index (TCI) and the vegetation health index (VHI) (Kogan, 1995). Often, these indices are used to assess drought and crop growth as well as to forecast early crop yields. For example, Jiang et al. (2021) used the NDVI, VCI, TCI and VHI to assess plant growth and drought conditions in the Jing-Jin-Ji region of China; Kogan et al. (2012) used the VCI and the VHI to forecast winter wheat, sorghum and corn yields from 3–4 mth before harvest in Kansas, USA. Kloos et al. (2021) monitored agricultural drought in Bavaria, Germany, using the TCI, the VCI and the VHI. Additionally, Luong and Bui (2023) investigated the use of the VCI, the TCI, the VHI and the temperature-vegetation dryness index (TVDI) to identify the indicator areas for predicting the winter–spring rice yield in the Central Highlands, Vietnam. These studies reported clear correlations between satellite-based vegetation indices and crop yields.

From the above reports, both meteorological drought indices and satellite-based vegetation indices have shown great potential for drought monitoring. However, the question remains unanswered regarding which indices are suitable for monitoring plant health and drought. In addition, the change in vegetation cover and the severity of drought depend on geographical and environmental factors such as land cover/land use (LULC) and soil types (Usman et al., 2013; Vicente-Serrano et al., 2020). Therefore, identifying areas sensitive to changes in rainfall and climate conditions helps to provide early warnings about drought and facilitates timely adaptation measures.

The Central Highlands of Vietnam, covering an area of 54,508 km^2, has a tropical monsoon climate region and

is heavily affected by the El Niño phenomenon (Van Viet, 2021). The region has a dry season from December to early May, during which only 10−15% of the total annual rainfall occurs, leading to severe droughts in recent years such as 2002, 2004−2005, 2010 and 2015−2016 (Dinh et al., 2022). Coffee and rice are the main crops in the Central Highlands, with coffee covering 5,825 km^2 and accounting for about 10% of the region's total area, making it the world's most concentrated coffee production area (Baker, 2016). Vietnam ranks as the world's second-largest coffee producer, with 86% of production from the Central Highlands (Tiemann et al., 2018). Coffee is highly sensitive to weather conditions and drought (Venancio et al., 2020; Byrareddy et al., 2021; Dinh et al., 2022); consequently, since 2014, drought has had a major impact on coffee production, affecting flowering and ripening processes and reducing yields by about 50% in severe drought years (Le Nguyen and Nguyen, 2018). Rice is cultivated on more than 1,500 km^2, providing food for 6 million people. It has two growing seasons: summer-autumn (May–September) and winter-spring (December–April) (Chung et al., 2015). The winter-spring season coincides with the dry period, resulting in large crop yield fluctuations due to water scarcity. Research from India and Thailand has demonstrated strong relationships between rice yields and meteorological factors (Raja et al., 2014; Prabnakorn et al., 2018), with both drought and humidity affecting yields (Lavane et al., 2023). Given the major impact of meteorological factors on coffee and rice yields, it is crucial to determine appropriate drought indices, time scales and lag times for early warning systems for the different crop types and local conditions.

With these considerations in mind, the current study aimed to identify the most suitable meteorological drought and vegetation indices for monitoring drought and grain crop and coffee yields in the Srepok River basin. The analysis included common meteorological drought indices (SPI, EDI), vegetation indices (VI; VCI, TCI, VHI) and coffee and winter-spring rice yields. The specific research objectives were: 1) analyzing the impact of drought on vegetation indices by 1a) analyzing the correlation between meteorological drought indices and vegetation indices for each LULC type in the Srepok River basin; and 1b) analyzing the differences in values of vegetation indices between dry and wet conditions; 2) identifying the appropriate meteorological drought index, vegetation index and indicator area for drought monitoring; 3) analyzing the correlation between meteorological drought indices at different time scales and lag times with coffee and rice yields; and 4) identifying the suitable meteorological drought index at the appropriate time scale and lag time for early yield warning of each crop type.

Materials and Methods

Study area

The Srepok River basin has an area of 30,942 km^2, with 18,162 km^2 in Vietnam and 12,780 km^2 are in Cambodia. It is a sub-basin of the Mekong River and is located in the Central Highlands of Vietnam. The area is situated between 11°45′–13°15′N and 107°15′–109°E, with an elevation range of 140–2,406 m (Fig. 1). The study area is in the tropical monsoon climate zone, with a climate divided into two seasons: the rainy season and the dry season. The rainy season lasts for 6 mth, from May to October, coinciding with the southwest monsoon period. The dry season occurs from November to April, with rainfall during this period accounting for approximately 10−25% of the total annual rainfall. This dry season often leads to water shortages for agriculture. The basin has a population of approximately 2.3 million people (GSO, 2018). Agriculture is the main economic activity in the area, with coffee and winter-spring rice as the primary crops. The region experiences frequent droughts due to its tropical monsoon climate, necessitating an evaluation of drought impacts on crop yields.

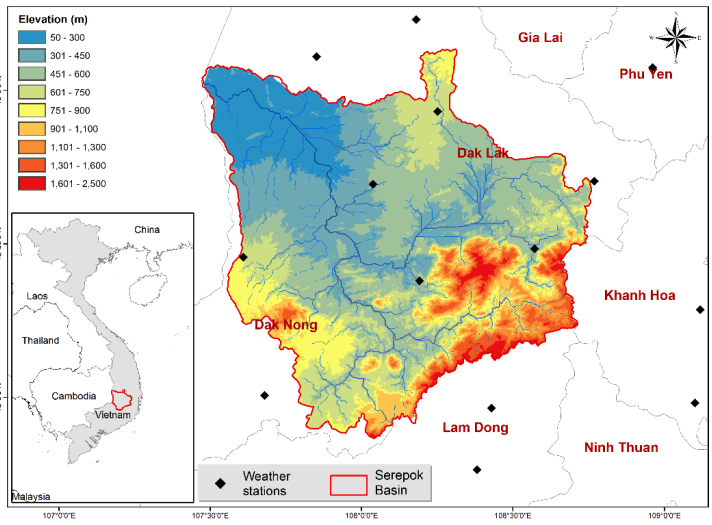

Fig. 1 Elevation map of the study area (Srepok River Basin in Vietnam), illustrating terrain variation from lowlands (50 m) to highlands (up to 2,500 m), overlaid with weather station locations. The basin spans the provinces of Dak Lak, Dak Nong and Lam Dong and borders Khanh Hoa. Inset map shows the basin's location within Vietnam.

Data

The analysis of the meteorological drought and vegetation indices was based on the rainfall data from 14 monitoring stations and NDVI and land surface temperature (LST) data from the Moderate Resolution Imaging Spectroradiometer (MODIS) products during the period 2000−2022. The rainfall data were collected from meteorological stations in the study area from 2000 to 2022 (Fig. 1). In total, 14 rainfall stations were included in the analysis, with 5 stations located in the Srepok area and 9 stations in the surrounding area.

The NDVI and LST data of the MODIS products were collected via the website https://earthexplorer.usgs.gov/. The NDVI data were extracted from the MODIS/Terra Vegetation Indices 16-Day L3 Global 500 m version 6 (MOD13A1 v006) product, which had a spatial resolution of 463 m × 463 m and a temporal resolution of 16 d. The LST data were taken from the MODIS/Terra Land Surface Temperature/ Emissivity 8-Day L3 Global 1 km version 6 (MOD11A2 v006) product, with a spatial resolution of 926.6 m × 926.6 m and a temporal resolution of 8 d. The data were processed to a common spatial and temporal resolution to ensure compatibility for analysis. Temporal resolution calculations were made on on a monthly basis. The monthly NDVI data were obtained using the maximum value composite method to reduce the impact of atmospheric conditions (Holben, 1986; Chu et al., 2019). The monthly average LST was calculated and resampled using the bilinear method to match the spatial resolution of NDVI.

The crop yield data for coffee and rice were collected at the district level from statistics compiled in offices of the Dak Lak, Dak Nong and Lam Dong provinces from 2000 to 2022. Additionally, a land use map of the Srepok Basin in 2015 was obtained from the Sub-National Institute of Agricultural Planning and Projection.

Methods

The overall workflow is illustrated in Fig. 2, with additional discussion below.

Meteorological drought indices and vegetation indices

The SPI was proposed by McKee et al. (1993). It is a widely used drought index that is based on the distribution of rainfall. The SPI is calculated at different time scales, from one to many months. Let x be the rainfall corresponding to the selected time step of any month in a year, then the SPI is calculated according to the following steps.

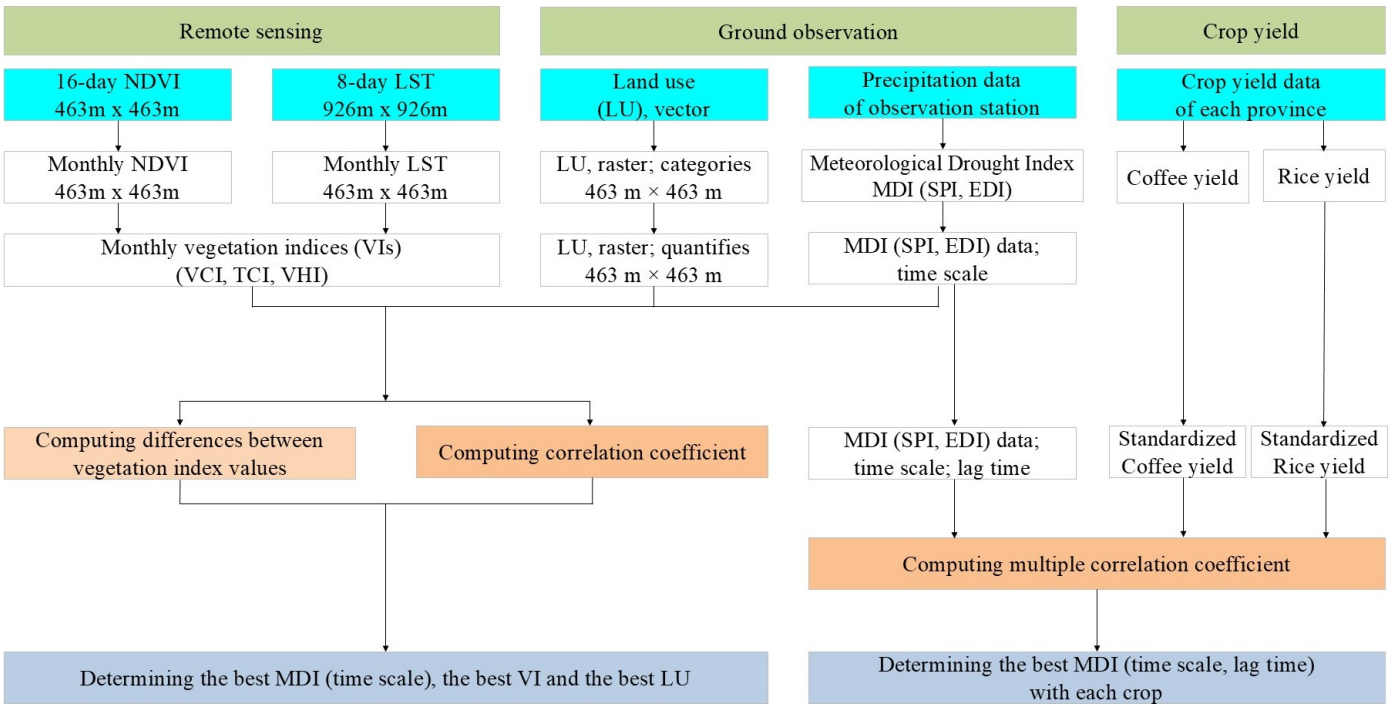

Fig. 2 Workflow diagram illustrating the integration of remote sensing data (NDVI, LST, and vegetation indices), ground observations (land use and precipitation-based drought indices), and provincial crop yield records to identify the most suitable meteorological drought indices (MDI), vegetation indices (VI), and land use categories for drought and crop yield monitoring in the Srepok River Basin, Vietnam.

Determine the shape parameter (b) based on Equation (1) and the scale parameter (a) based on Equation (2), according to a gamma distribution:

$$\beta = (1+ \sqrt{1+4U / 3}) / 4U \quad (1)$$

$$\alpha = \bar{X} / \beta \quad (2)$$

where $\bar{X}$ is the average value of X and U is a statistical coefficient, defined using Equation (3):

$$U = ln(\bar{X}) - (ln(X) / n \quad (3)$$

where n is the number of precipitation observations.

The gamma distribution function was calculated using Equation (4):

$$G(x) = (\int_0^x x^{(\alpha - 1)} e^{((-x)/\beta)} dx)/(\beta^{\alpha} \Gamma(\alpha)) \quad (4)$$

where G(a) = (a - 1)!. Since the gamma function is not defined for x = 0, and the precipitation distribution can contain zeros, the cumulative probability was used, as shown in Equation (5):

$$H(x) = q + (1 - q)G(x) \quad (5)$$

where q is the probability corresponding to x = 0.

The SPI was defined based on transforming the cumulative probability H(x) into a standardized random variable with a mean of zero (Equation 6) and a variance of one, as shown in (Equation 7):

$$\begin{aligned} SPI &= (2{,}515517 + 0{,}802583t + 0{,}010328t^2)/ \\ &\quad (1 + 1{,}432788t + 0{,}189269t^2 + 0{,}001308t^3) - t \qquad 0<H(x)\leq 0{,}5 \\ SPI &= t-(2{,}515517+0{,}802583t+0{,}010328t^2)/ \\ &\quad (1+1{,}432788t+0{,}189269t^2+0{,}001308t^3) \qquad 0{,}5<H(x)\leq 1 \end{aligned} \quad (6)$$

where

$$\begin{aligned} t &= \sqrt{\ln (1 / (H(x)^2))} \qquad 0 < H(x) \leq 0{,}5 \\ t &= \sqrt{\ln (1 / (1 - H(x))^2))} \qquad 0{,}5 < H(x) \leq 1 \end{aligned} \quad (7)$$

The gamma distribution function was calculated using the subroutine 'cdfgam' in the Cdflib.f90 package from the Florida State University website (https://people.sc.fsu.edu/~jburkardt/f_src/cdflib/cdflib.html).

The EDI, as proposed by Byun and Wilhite (1999), is a function of the precipitation needed for a return to normal (PRN) and was calculated using Equation (8):

$$EDI_j = PRN_j / ST(PRN_j) \quad (8)$$

where

$$PRN_i = DEP_i / (\sum_{k=1}^{j}(1/k)) \quad (9)$$

$$DEP = EP - MEP \quad (10)$$

and j is the calculation time, *ST(PRN)* is the standard deviation of *PRN*, *EP* is the effective rainfall and *MEP* is the average value of each *EP* day. Once the time step had been set, the daily *EP* was calculated according to Equation (11):

$$EP_i = \sum_{n=1}^{i}[(\sum_{m=1}^{n} P_m) / n] \quad (11)$$

where i is the calculation period and P_m is the rainfall on day m - 1 (the day before). Daily rainfall data were used for calculating the *EDI*, so it was necessary to average the daily values to calculate the monthly *EDI*.

Next, the *SPI* and *EDI* calculated for each station were interpolated using the IDW method to obtain a raster layer with a spatial resolution of 463 m × 463 m. These two indices were constructed for time scales from 1 mth to 13 mth.

VCI is the normalized value of NDVI over time (F.N. Kogan, 1995), according to Equation (12):

$$VCI = 100* (NDVI_i - NDVI_{min}) / (NDVI_{max} - NDVI_{min}) \quad (12)$$

where $NDVI_i$ is the *NDVI* value of a particular pixel in a certain year at time i, while $NDVI_{max}$ and $NDVI_{min}$ are the maximum and minimum NDVI values, respectively, over a period of analysis. The numerator represents the difference between the actual and minimum values of the NDVI and reflects the state of plant growth and meteorological conditions. The denominator's maximum and minimum values indicate the best and worst conditions, respectively, of change and partly reflect the local vegetation's condition. Hence, the VCI encompasses both historical and real-time information about the NDVI. The VCI ranges from 0 to 100, with lower values indicating underdeveloped plants and higher levels of drought. In the current study, the VCI was calculated for each month from 2000 to 2022.

The TCI was created by Kogan (1995) and represents the normalized value of LST over time, as shown in Equation (13):

$$TCI = 100* (LST_{max} - LST_i) / (LST_{max} - LST_{min}) \quad (13)$$

The VHI was developed to assess plant health based on a combination of the VCI and the TCI (Kogan, 2001), as shown in Equation (14):

$$VHI = \propto VCI + (1 - \propto)TCI \quad (14)$$

The *VHI* combines the information from the *NDVI* and the *LST*, with the weight α typically set to 0.5, to evaluate the health of vegetation.

Selecting a vegetation index and meteorological drought index pair for crop monitoring

The criteria for selecting a vegetation index and meteorological drought index pair was based on the best Pearson's correlation coefficient, with a clear difference in the vegetation index values between dry and wet conditions.

Calculating difference in vegetation index value between dry and wet conditions

Drought and wetness were determined by the meteorological drought indices SPI and EDI. Typically, thresholds such as -1, -1.5 and -2 represent drought levels ranging from mild, to severe and to extremely severe, respectively, while thresholds of 1, 1.5 and 2 represent wetness levels ranging from slightly wet, to wet to extremely wet, respectively. There was a substantial difference in the duration of drought and wetness from applying these thresholds in the Srepok basin. In addition, for simplicity, water availability was classified into three groups: drought, normal and wet. In a drought month, the drought indices were less than or equal to the 25th percentile. Conversely, in a wet month, the drought indices were greater than or equal to the 75th percentile.

Determining correlation between drought and vegetation indices

Pearson's correlation coefficient was used to determine the correlation between the meteorological drought index and the vegetation index, which was subsequently used as an indicator of the impact of meteorological drought on vegetation. The values of these indices can be based on grid cells or averaged by land use type. In this case, the length of the time series was equal to the number of years analyzed (23 yr).

The vegetation index with the highest Pearson correlation coefficient was considered a suitable index for drought assessment. In addition, because the vegetation indices of different crop groups have different sensitivities to rainfall variability, the correlation coefficient was determined separately for each LULC type. The crop group with the highest correlation coefficient was selected as the indicator crop.

Determining correlation between drought index and crop yield and selecting monitoring index for crop yield

Hiep et al. (2023) reported that perennial agriculture (PeA) and paddy rice (PdR) were easily damaged by drought. PeA in this area includes coffee, cashew, pepper and Macca, of which robusta coffee is the main crop. In the past 20 years, coffee yields in this area have tended to increase due to investments in seed, fertilizer, water sources and improved agricultural techniques (Van Viet and Thuy, 2023). In addition, according to Hiep et al. (2023), the trends in the vegetation indices in this area were quite clear. Taking these trends into account, instead of the Pearson's correlation coefficient, the current study used a multiple correlation coefficient between crop yields or vegetation indices (y) with meteorological drought index (x) and a time variable (t). The meteorological drought index along with its time scale with the highest multiple correlation coefficient was considered as a suitable index for drought monitoring. This coefficient was determined using Equation (15):

$$R_{y.xt} = \sqrt{(r_{yx}^2 + r_{yt}^2 - 2r_{yx}\, r_{yt}\, r_{xt}) / (1 - r_{xt}^2)} \quad (15)$$

where r_{yx}, r_{yt} and r_{xt} are the Pearson's correlation coefficients between y and x, y and t, and x and t, respectively.

The analysis of the impact of drought on crop yields used values averaged by district of the yield (y) and the drought index (x). There were 19 districts within the basin. Furthermore, when analyzing separately for each district, the length of the series in Equation 15 was $n = 23$ (23 yr). The data from the districts were combined into a single series to ensure the stability of the results. Therefore, the length of the analysis series was $n = 19 \times 23 = 437$. The y values between districts were compared based on standardization to the same mean value of 0 and SD value of 1.

Results and Discussion

Impact of drought on vegetation

The study analysis aimed to identify drought-sensitive crops or crop groups and the most suitable meteorological and remote sensing drought index pairs for monitoring land cover status.

Difference in remote-sensing vegetation index values between dry and wet conditions

The results of determining the difference in vegetation index value between dry and wet conditions by land cover types are presented in Fig. 3 based on the limits for the dry and wet conditions corresponding to the threshold values of the 25th and 75th percentiles, respectively; excluding the blue areas, there were significant (p = 0.01) differences in the vegetation index values between the dry and wet conditions.

As shown in Fig. 3, the vegetation indices under conditions determined using the SPI were generally higher than those determined based on the EDI. The difference was most evident for the VHI. Based on these results, the SPI was a good indicator of the wetness conditions and plant health. In addition, Fig. 3 shows that PeA was most sensitive to wetness conditions, with natural forests being less affected by drought.

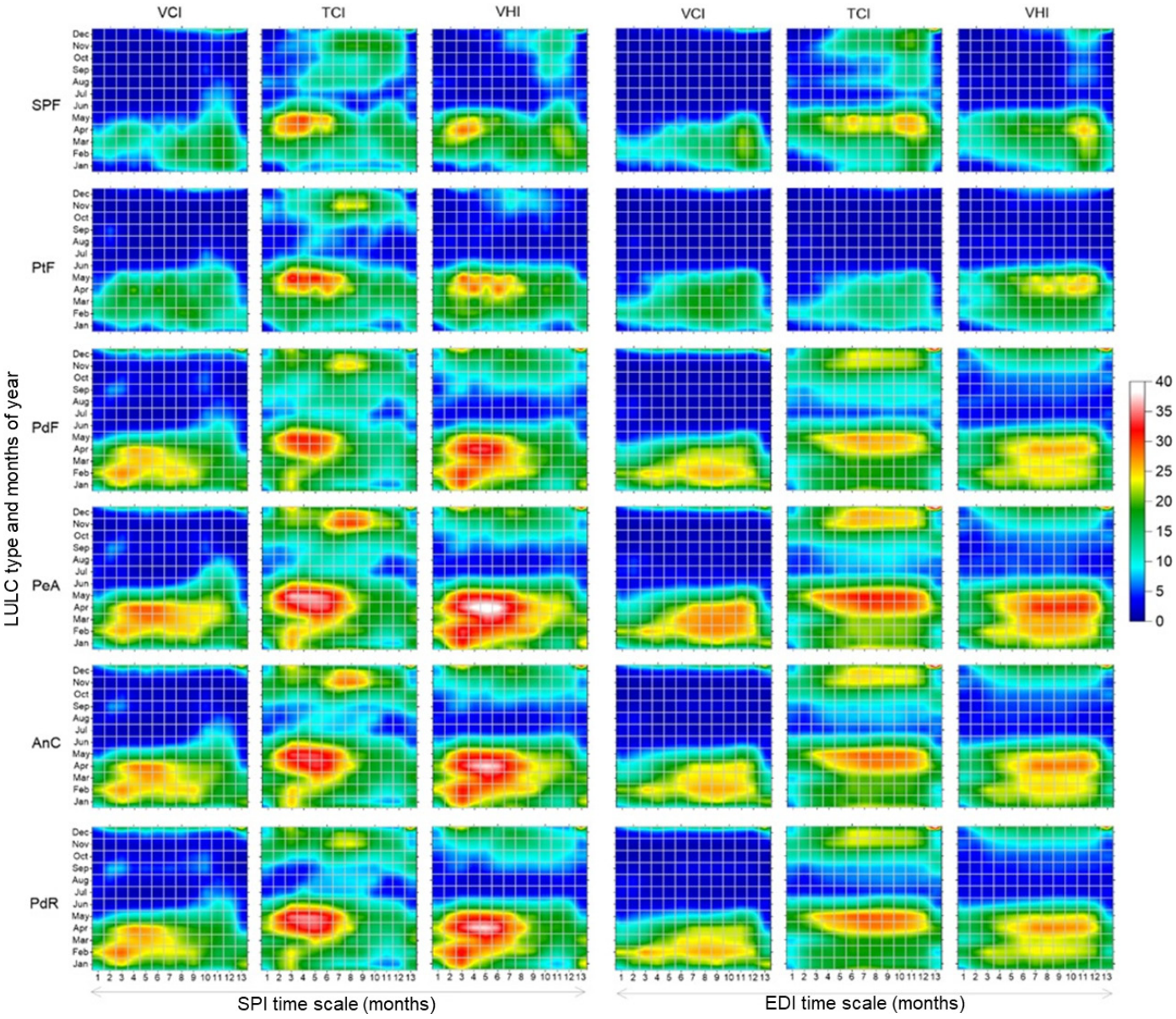

Fig. 3 Differences between vegetation index values for dry and wet conditions, based on standardized precipitation index (SPI) and effective drought index (EDI), where abbreviations for different land use/land change (LULC) types are provided in Table 1

Table 1 Summary of land use andland cover types

Land use/land cover type	Abbreviation	Area (km^2)	Area (%)
Perennial agriculture	PeA	3400	28.9
Special-use forest	SpF	2367	20.1
Production forest	PdF	1970	16.8
Annual crops	AnC	911	7.7
Protection forest	PtF	868	7.4
Paddy rice	PdR	508	4.3

Correlation coefficient analysis between meteorological drought indices and vegetation indices

The Pearson's correlation coefficient values between vegetation indices by LULC type and the meteorological drought index at different time scales are shown in Fig. 4.

Based on the results, the vegetation indices in coffee-growing areas had the highest correlation coefficients, indicating that they were the most sensitive to rainfall variability. The crops consisting of protection forest (PtF), production forest (PdF), annual crops (AnC) and paddy rice (PdR) all had similar characteristics regarding the effects of rainfall variability on their condition. Furthermore, as with this crop group, special-use forests were affected by drought but with a different distribution.

Both the EDI and SPI showed that the effects of rainfall variability only had a significant impact on vegetation indices in the period from January to May, with the most significant impact from February to April (Fig. 3 and Fig. 4). This was because February–April are the dry season months, when the effect of drought can be severe if it follows a lack of rainfall at the end of the previous rainy season.

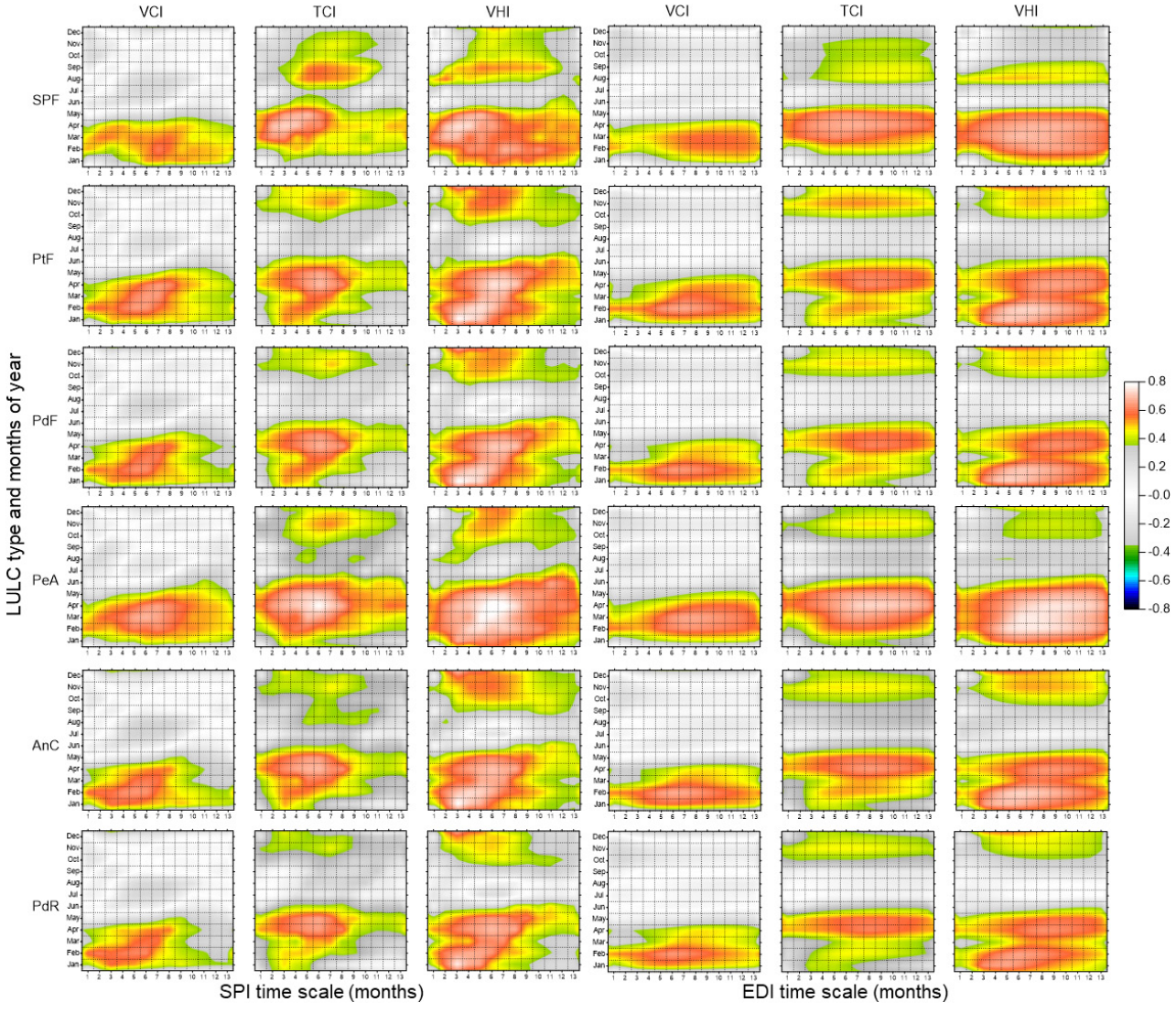

Fig. 4 Pearson's correlation coefficient for standardized precipitation index (SPI) and effective drought index (EDI) by land use/land cover type and drought index on time scales from 1 mth to 13 mth, where gray areas indicate $p \leq 0.01$

In addition, the correlation coefficient was usually high from February to April for the VCI, while it was usually high in April and May for the TCI. This may have been be related to: 1) the end of the dry season from February to April; 2) the high temperature base in April and May (Fig. 5b), due to the sun passing through its zenith; and 3) the effects of the lack of rainfall at the end of the previous year's rainy season on the land cover at the end of the dry season in the following year.

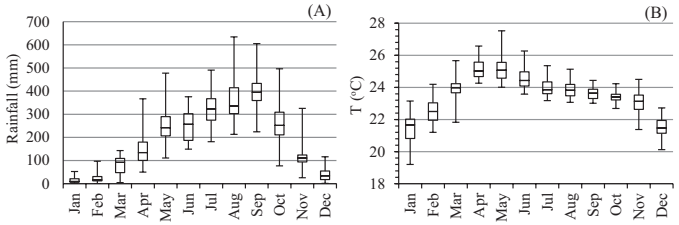

Fig. 5 Climatic data for Serepok basin region: (A) precipitation; (B) temperature, where the horizontal line within each box indicates the median, while the upper and lower edges of the box represent the 75th and 25th percentiles, respectively, and the upper and lower ends of the whiskers represent the maximum and minimum values

Compared to the VCI and the TCI, the VHI had a better relationship with both the EDI and the SPI. In addition, the VHI reflected the impact of drought on vegetation over a longer period (from February to May). Therefore, the VHI was the best choice among these vegetation indices for assessing the vegetation health caused by rainfall variability. In addition, Van Viet & Thuy (2023) reported that coffee yields in this area had a better relationship with the VHI compared to the VCI and the TCI, supporting the choice of the VHI.

A comparative analysis of Fig. 3 and Fig. 4 revealed notable similarities. Specifically, similar results were produced from using correlation analysis and difference analysis according to wet and dry phases in selecting remote sensing indices. The correlation analysis used the complete dataset, while the phase analysis used only a part of the dataset. Therefore, the reliability of the correlation analysis would be expected to be better.

The most suitable meteorological drought index and its time scale for monitoring crop conditions in this area were determined using analysis of correlation coefficients between the drought and vegetation indices from February to May, when they had the strongest relationship. With these months, the analyzed series had a length of 4 (months) × 23 (years) = 92. Fig. 6 illustrates the relationship between the VHI with the SPI based on 1 mth data (SPI1) and the SPI based on 5 mth data (SPI5). Fig. 7 summarizes the correlation coefficients between vegetation indices of some LULC types with the SPI and the EDI. Due to the similar characteristics of the LULC types, only the data for PeA and AnC are presented.

According to Fig. 7, the SPI had a higher correlation coefficient and a more pronounced peak than the EDI. Although the difference in correlation coefficients was not significant, the SPI was still a better choice than the EDI. Notably, SPI6 had the highest correlation, indicating that SPI6 was the best choice for assessing the impact of meteorological drought on vegetation conditions, which aligned with other studies in this basin regarding the effects of drought(Sam et al., 2019; Tram et al., 2021). Since the vegetation indices used for analysis were from February to May, SPI6 in this case was calculated from the rainfall starting in September, as the month with the highest rainfall (Fig. 5A), to May in the following year.

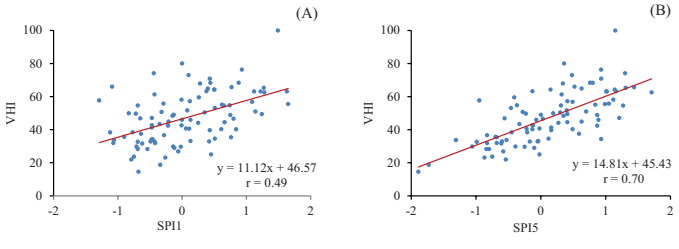

Fig. 6 Correlation coefficients (r) for vegetation health index (VHI) on perennial agriculture area with: (A) standardized precipitation index (SPI) based on 1 mth data (SPI1); (B) SPI based on 5 mth data (SPI5)

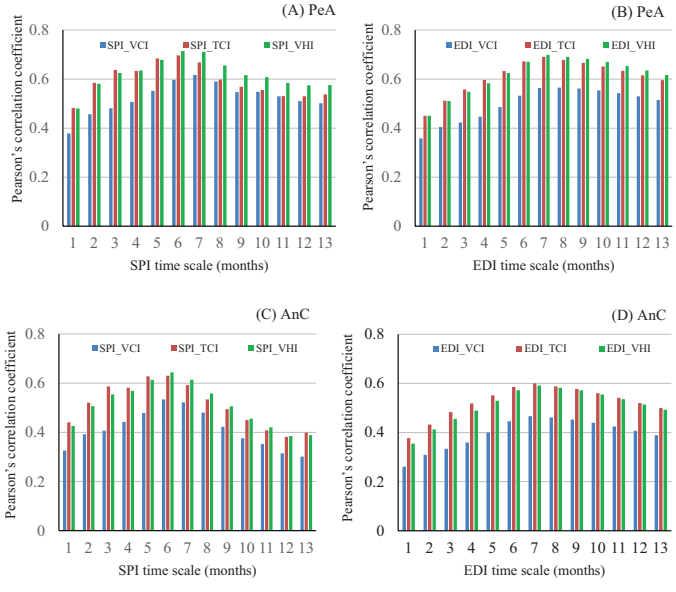

Fig. 7 Correlation coefficients (r) between vegetation indices (VHI, VCI, TCI) in perennial agriculture (PeA) and annual crop (AnC) areas and meteorological drought indices (SPI, EDI) (p = 0.01)

The vegetation indices for February and March were both related to rainfall from September to November. Since rainfall from December to March was not substantial, the vegetation indices for April and May were related to the rainfall in these two months. Similarly, Fig. 4 and Fig. 7 showed that the relationship between vegetation indices with an increase in the meteorological drought index, in the order TCI, VCI, VHI. Thus, the pair of VHI and SPI6 was the most suitable for drought monitoring in this area.

The results from determining the correlation coefficient between the VHI and SPI6 in the drought-sensitive period from February to May by grid cells are shown in Fig. 8A. The results from overlaying this with the LULC map (Fig. 8B) showed that the correlation coefficient was often low outside the coffee-growing area and high within. The mean and SD values of the correlation coefficients for the main LULC types are shown in Table 2.

Comparing the correlation coefficient values in Table 2 were quite low, compared to the values in Figs. 7A and 7CF for SPI6, due to the difference in the input data in the calculation of the correlation coefficient. In particular, the results in Fig. 7 were calculated based on the average data for each LULC, while the results in Table 2 were based on the calculation using each grid cell. Due to the small area of a grid cell, the associated data were often unstable, which resulted in a low correlation coefficient.

According to Table 2, the degree of impact of drought on VHI increased in the order special-use forest (SpF), PtF, PdF, PdR, AnC, PeA. The first group (SpF, PtF and PdF) had a low correlation with the SPI. This group contains woody trees with well-developed roots and high coverage, so they were less affected by drought. In this group, SpF was the primary forest with the highest coverage, as well as being the least affected by drought. The low SD value (Table 2) indicated that the spatial impact of drought on SpF was quite uniform.

The remaining group (PdR, AnC and PeA), was sensitive to drought because each member involved water-loving crops with short roots. PeA in this area included coffee, cashew, pepper and Macca, with robusta coffee being the main crop. Coffee is a water-loving crop and is sensitive to high temperatures. Often, drought is associated with high temperatures, which makes coffee more susceptible to adverse drought impacts. AnC in this area included corn, cassava, vegetables, soybeans, peanuts, sweet potatoes and sugarcane. While some of these crops have better drought tolerance than PeA, overall there was not much difference. PdR was the main food crop in this area. It was given priority care and was also often located in places with convenient water sources. Therefore, compared to PeA and AnC, it was less affected by drought.

Table 2 Summary statistics of Pearson's correlation coefficients (r) between vegetation health index and standardized precipitation index by land use land cover type ($p = 0.01$)

Land use land cover type	Abbreviation	Mean	SD
Special-use forest	SpF	0.31	0.06
Protection forest	PtF	0.36	0.1
Production forest	PdF	0.39	0.12
Paddy rice	PdR	0.44	0.11
Annual crops	AnC	0.46	0.13
Perennial agriculture	PeA	0.49	0.11

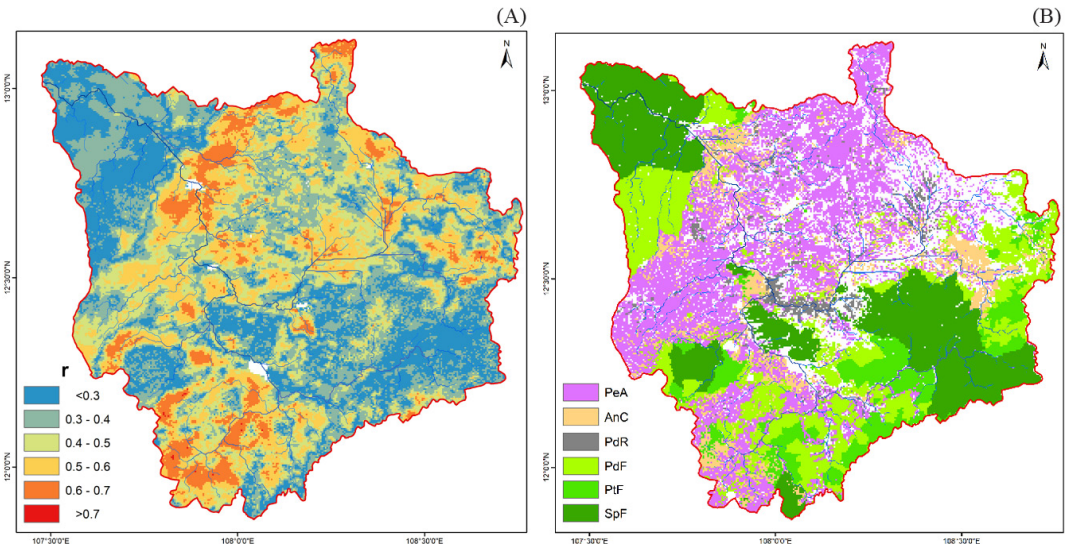

Fig. 8 (A) Correlation coefficient (r) between SPI based on 6 mth data (SPI6) and VHI during the period from February to May ($p = 0.01$); (B) spatial distribution of main land use land cover types (defined in Table 1)

Relationship between coffee yield and meteorological drought indices

According to Table 2 and Fig. 8, the vegetation index in the coffee-growing areas was the most sensitive to rainfall fluctuations. In other words, droughts significantly affected the coffee yield. The relationship between coffee yield and each meteorological drought index was determined based on the multiple correlation coefficient. The multiple correlation coefficient was determined for different time scales of the meteorological drought indices and the time at which it is taken before harvest (the lag time). In addition, to increasing the reliability of the analysis, the data for calculating the multiple correlation coefficient was connected between districts to create a longer series. Fig. 9A illustrates the preparation of data for calculating the multiple correlation coefficient with SPI3 at a lag time of 10 months ($SPI3_{-10}$).

The results of calculating the multiple correlation coefficient (R) between coffee yield, the time variable and the meteorological drought indices (SPI and EDI) are shown in Figs. 9B and 9C, respectively. Based on these results, the notable characteristics were: 1) the SPI had a higher correlation coefficient than EDI; 2) the SPI at a time scale of 5 mth and a lag time of 9 mth ($SPI5_{-9}$) and the EDI at a time scale of 6 mth and a lag time of 9 mth ($EDI6_{-9}$) had the highest correlation coefficient. The difference in the time scales of the SPI and the EDI for the highest correlation coefficient was due to the difference in the way these indices were calculated.

Because coffee was harvested in October, $SPI5_{-9}$ was calculated from the precipitation from September to January in the year of harvest, while $EDI6_{-9}$ was calculated based on the precipitation from August to January. These results showed that precipitation from the middle of the rainy season to the beginning of the dry season was an important factor contributing to the coffee yield. According to Fig. 9B, the highest multiple correlation coefficient did not differ significantly between $SPI3_{-9}$ and $SPI5_{-9}$, indicating that the rainfall from November to January in the harvest year played the most important role, with the rainfall from September and October of the previous year having a lower impact on the yield. The average rainfall during these three months was only 166 mm and accounted for 7.2% of annual rainfall (Fig. 5A); nonetheless, it determined the soil moisture condition and the ability to irrigate coffee during these months, as well as the following dry months. The analysis of the multiple correlation coefficient between coffee yield, the time variable and SPI1 or EDI1 showed that this coefficient (significant at the 0.01 level), decreased in the order November, October, September, December of the previous year and then January of the harvest year (Fig. 10). Thus, November rainfall was the most important for coffee yield.

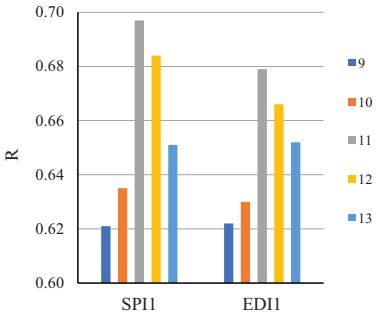

Fig. 10 Multiple correlation coefficient (R) between standardized coffee yield, time variable and SPI based on 1 mth data (SPI1) or EDI based on 1 mth data (EDI1) taken from previous September to January of harvest year

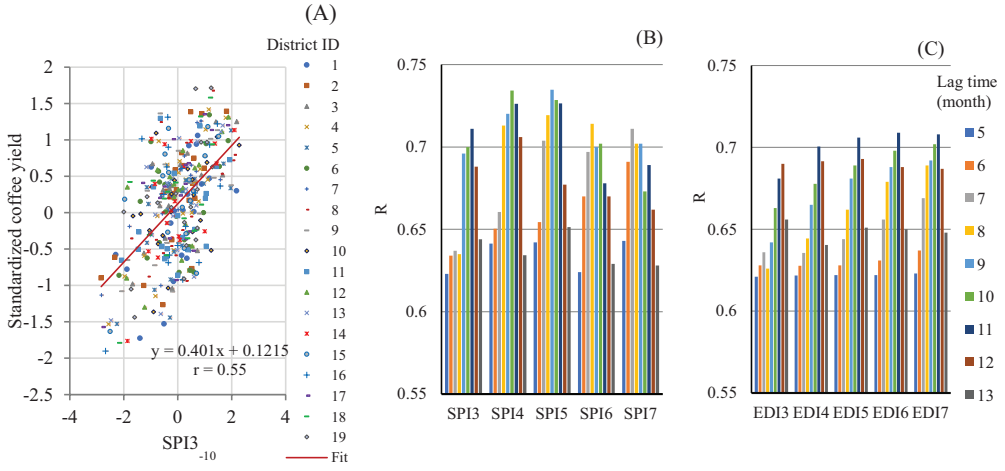

Fig. 9 (A) Simple correlation coefficient (r) between standardized coffee yield and SPI3 at a lag time of 10 mth; (B) multiple correlation coefficient (R) between standardized coffee yield, time variable and SPIx; (C) multiple correlation coefficient (R) between standardized coffee yield, time variable and EDIx, where SPIx and EDIx represent the standardized precipitation index and effective drought index, respectively, with scale time x ranging from 3 to 7 mth. All correlations are significant at the 0.01 level

From the above results, $SPI5_{-9}$ may be prioritized to analyze the impact of drought on coffee productivity in this area. Because $SPI5_{-9}$ had a positive (and quite high) correlation coefficient with crop yield, a lack of rainfall during the period from September to January may seriously affect the coffee yield. These findings were quite consistent with the study by Viet and Thuy (2023), which used vegetation health indices to forecast the coffee yield in this region.

Relationship between winter-spring rice yield and meteorological drought indices

The Srepok River basin has two main rice seasons (winter-spring and summer-autumn). Since only the winter-spring season was significantly affected by drought, the analysis below has focused on this season. Usually, the winter-spring rice season in the Srepok River basin begins in early December and ends in late March. Similar to coffee, the multiple correlation coefficient between rice yield, the time variable and meteorological drought indices was constructed to analyze the effects of drought on rice yield. Drought indices at different time scales were taken from 1 mth to a few months before harvest. The results, which were significant at the 0.01 level, are shown in Fig. 11.

A comparison of Figs. 7a, 7c and Fig. 4 showed that the role of meteorological drought indices for rice and coffee was similar. In addition, SPI5 had the highest multiple correlation coefficient when it was taken 3 mth before harvest ($SPI5_{-3}$), indicating that rainfall from August to December had the best relationship with the yield of winter-spring rice. Because winter-spring rice was harvested in March, $SPI5_{-3}$ related to the rainfall from August to January. This period coincided with the period when the coffee yield was readily affected by drought (from September to January), as mentioned above. These findings were consistent with other studies conducted in the Mekong Delta, Vietnam and the Eastern Indian state of Odisha, which reported similar results (Raja et al., 2014; Lavane et al., 2023).

It can be seen that rainfall in the period from September to January was closely related to the yield of both coffee and rice. The total rainfall in the winter-spring rice season in this basin averaged about 240 mm, which was only 50% of the reference evaporation and much lower than the water requirement of rice. To meet the water requirement of rice, the remaining water was taken from the surface water that was stored during the rainy season, especially from September to the beginning of the dry season.

Overall, the results revealed that: 1) the EDI was not a priority option for monitoring rice and coffee yields; 2) SPI5 had the highest correlation coefficient with coffee and winter-spring rice; and 3) rainfall from the middle of the rainy season to the beginning of the dry season was decisive in achieving good yields of coffee and winter-spring rice.

Conclusion

Suitable meteorological drought and vegetation indices were identified for monitoring drought impacts in the Srepok River basin. Both statistical analyses of dry-wet phases and correlation analyses demonstrated that rainfall deficits significantly affected vegetation conditions and crop yields, leading to the assessment of their relationships and performance.

Of the meteorological drought indices, the SPI had stronger correlations with vegetation indices, coffee yield and winter-spring rice yield than the EDI, making the former a better choice for drought monitoring and yield prediction. Among the vegetation indices, the VHI performed best, highlighting its suitability for drought assessment.

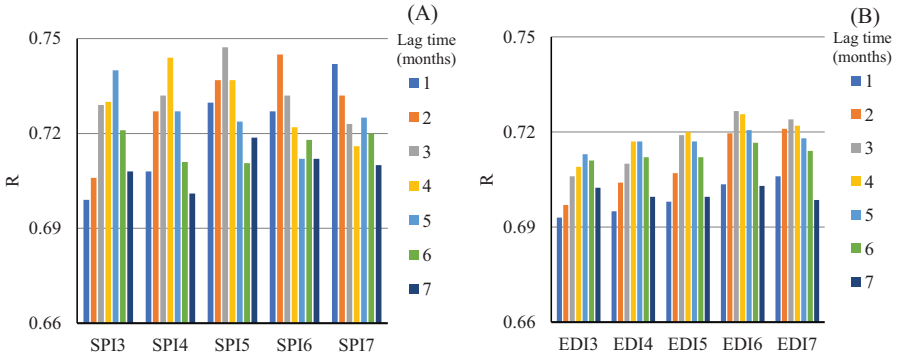

Fig. 11 Multiple correlation coefficients (R) between normalized rice yield, time variable and (A) the standardized precipitation index (SPI); (B) effective drought index (EDI)

Regarding time scales, SPI6 showed a strong relationship with the VHI from February to May, confirming this pair as optimal for drought monitoring. The period from February to early May was most affected by drought, influenced by rainfall variations from the previous September, especially between February and April.

The impact of drought on the VHI increased in the order SpF, PtF, PdF, PdR, AnC, PeA, with PeA being most sensitive to rainfall fluctuations, making it a key indicator for drought assessment.

For coffee yield, SPI5 at 9 mth before harvest had the highest correlation, emphasizing rainfall from September to January—especially in November and October—as critical factors. Similarly, for the winter-spring rice yield, SPI5 at 3 mth before harvest was most effective, confirming its suitability for forecasting yields of both perennial and annual crops.

This study had some limitations due to the small number of vegetation and meteorological drought indices used in the analysis. Other indices need to be considered for inclusion in further studies.

Conflicts of Interest

The authors declare no conflict of interest.

Acknowledgments

The authors express their gratitude to the Industrial University of Ho Chi Minh City (IUH) for the financial support provided for this study under grant number 100/HĐ-ĐHCN. The authors would also like to express special thanks and remembrance to Assoc. Prof. Dr Dao Nguyen Khoi, whose comments substantially improved the manuscript.

References

AghaKouchak, A., Farahmand, A., Melton, F.S., Teixeira, J., Anderson, M.C., Wardlow, B.D., Hain, C.R. 2015. Remote sensing of drought: Progress, challenges and opportunities. Rev. Geophys. 53: 452-480. doi.org/10.1002/2014RG000456

Anshuka, A., Buzacott, A.J., Vervoort, R.W., van Ogtrop, F.F. 2021. Developing drought index-based forecasts for tropical climates using wavelet neural network: An application in Fiji. Theor. Appl. Climatol. 143: 557-569. doi.org/10.1007/s00704-020-03446-3

Baker, P.S. 2016. Coffee and climate change in the Central Highlands of Vietnam. Coffee&Climate, Hanns R. Neumann Stiftung, Germany.

Bhunia, P., Das, P., Maiti, R. 2019. Meteorological drought study through SPI in three drought prone districts of West Bengal, India. Earth Syst. Environ. 4: 43-55. doi.org/10.1007/s41748-019-00137-6

Byrareddy, V., Kouadio, L., Mushtaq, S., Kath, J., Stone, R. 2021. Coping with drought: Lessons learned from robusta coffee growers in Vietnam. Clim. Serv. 22: 100229.

Byun, H.R., Wilhite, D.A. 1999. Objective quantification of drought severity and duration. J. Clim. 12: 2747−2756.

Chu, H., Venevsky, S., Wu, C., Wang, M. 2019. NDVI-based vegetation dynamics and its response to climate changes at Amur-Heilongjiang River Basin from 1982 to 2015. Sci. Total Environ. 650: 2051−2062.

Chung, N.T., Jintrawet, A., Promburom, P. 2015. Impacts of seasonal climate variability on rice production in the Central Highlands of Vietnam. Agric. Agric. Sci. Procedia 5: 83-88.

Deo, R.C., Byun, H.R., Adamowski, J.F., Begum, K. 2016. Application of effective drought index for quantification of meteorological drought events: A case study in Australia. Theor. Appl. Climatol. 128: 359−379.

Dinh, T.L.A., Aires, F., Rahn, E. 2022. Statistical analysis of the weather impact on robusta coffee yield in Vietnam. Front. Environ. Sci. 10: 820916.

GSO. 2018. Statistical Yearbook of Vietnam 2018. Vietnam: Statistical Publishing House.

Haile, G.G., Tang, Q., Li, W., Liu, X., Zhang, X. 2020. Drought: Progress in broadening its understanding. Wiley Interdiscip. Rev. Water 7: e1407.

Hamal, K., Sharma, S., Khadka, N., Haile, G.G., Joshi, B.B., Xu, T., Dawadi, B. 2020. Assessment of drought impacts on crop yields across Nepal during 1987–2017. Meteorol. Appl. 27: e1950.

Hiep, N.V., Thao, N.T.T., Viet, L.V., Luc, H.C., Ba, L.H. 2023. Affecting [*sic*] of nature and human activities on the trend of vegetation health indices in Dak Nong province, Vietnam. Sustainability 15: 5695.

Himanshu, S., Singh, G., Kharola, N. 2015. Monitoring of drought using satellite data. Int. J. Earth Sci. 3: 66-72.

Holben, B.N. 1986. Characteristics of maximum-value composite images from temporal AVHRR data. Int. J. Remote Sens. 7: 1417−1434.

Holben, B.N., Tucker, C.J., Fan, C.J. 1980. Spectral assessment of soybean leaf area and leaf biomass. Photogramm. Eng. Remote Sens. 46: 651-656.

Huang, Y.F., Ang, J.T., Tiong, Y.J., Mirzaei, M., Amin, M.Z.M. 2016. Drought forecasting using SPI and EDI under RCP-8.5 Climate Change Scenarios for Langat River Basin, Malaysia. Procedia Eng. 154: 710-717.

Jain, V.K., Pandey, R.P., Jain, M.K., Byun, H.R. 2015. Comparison of drought indices for appraisal of drought characteristics in the Ken River Basin. Weather Clim. Extremes 8: 1−11.

Jiang, R., Liang, J., Zhao, Y., Wang, H., Xie, J., Lu, X., Li, F. 2021. Assessment of vegetation growth and drought conditions using satellite-based vegetation health indices in Jing-Jin-Ji region of China. Sci. Rep. 11: 13775.

Khoi, D.N., Sam, T.T., Loi, P.T., Hung, B.V., Nguyen, V.T. 2021. Impact of climate change on hydro-meteorological drought over the Be River Basin, Vietnam. J. Water Clim. Change 12: 3159−3169.

Kim, D.W., Byun, H.R., Choi, K.S. 2009. Evaluation, modification, and application of the effective drought index to 200-year drought climatology of Seoul, Korea. J. Hydrol. 378: 1−12.

Kloos, S., Yuan, Y., Castelli, M., Menzel, A. 2021. Agricultural drought detection with MODIS based vegetation health indices in southeast Germany. Remote Sens. 13: 3907.

Kogan, F., Salazar, L., Roytman, L. 2012. Forecasting crop production using satellite-based vegetation health indices in Kansas, USA. Int. J. Remote Sens. 33 : 2798−2814.

Kogan, F.N. 1995. Droughts of the late 1980s in the United States as derived from NOAA polar-orbiting satellite data. Bull. Am. Meteorol. Soc. 76: 655-668.

Kogan, F.N. 2001. Operational space technology for global vegetation assessment. Bull. Am. Meteorol. Soc. 82: 1949−1964.

Lavane, K., Kumar, P., Meraj, G., et al. 2023. Assessing the effects of drought on rice yields in the Mekong Delta. Climate 11: 13.

Le Nguyen, P., Nguyen, M.D. 2018. Drought adaptation and coping strategies among coffee farmers in the central highlands of Vietnam.

Leng, G., Tang, Q., Rayburg, S. 2015. Climate change impacts on meteorological, agricultural and hydrological droughts in China. Global Planet. Change 126: 23−34.

Luong, V.V., Bui, D.H. 2023. Determination of the most suitable indicator area and remote-sensing-based indices for early yield warning for winter-spring rice in the Central Highlands, Vietnam. J. Appl. Remote Sens. 17: 014504. https://doi.org/10.1117/1.JRS.17.014504.

Manatsa, D., Mukwada, G., Siziba, E., Chinyanganya, T. 2010. Analysis of multidimensional aspects of agricultural droughts in Zimbabwe using the Standardized Precipitation Index (SPI). Theor. Appl. Climatol. 102: 287−305.

McKee, T.B., Doesken, N.J., Kleist, J. 1993. The relationship of drought frequency and duration to time scales. Proc. 8th Conf. Appl. Climatol. 17: 179−183.

Mishra, A.K., Singh, V.P. 2010. A review of drought concepts. J. Hydrol. 391: 202−216.

Miyan, M.A. 2015. Droughts in Asian least developed countries: Vulnerability and sustainability. Weather Clim. Extremes 7: 8−23.

Mukherjee, S., Aadhar, S., Stone, D., Mishra, V. 2018. Increase in extreme precipitation events under anthropogenic warming in India. Weather Clim. Extremes 20: 45-53.

Palmer, W.C. 1965. Meteorological drought. US. Weather Bureau Res. Paper 45: 1-58.

Prabnakorn, S., Maskey, S., Suryadi, F., de Fraiture, C. 2018. Rice yield in response to climate trends and drought index in the Mun River Basin, Thailand. Sci. Total Environ. 621: 108−119.

Prajapati, V., Khanna, M., Singh, M., Kaur, R., Sahoo, R., Singh, D. 2021. Evaluation of time scale of meteorological, hydrological and agricultural drought indices. Nat. Hazard. 109 : 89−109.

Raja, R., Nayak, A., Panda, B., et al. 2014. Monitoring of meteorological drought and its impact on rice (*Oryza sativa* L.) productivity in Odisha using standardized precipitation index. Arch. Agron. Soil Sci. 60: 1701−1715.

Sam, T.T., Khoi, D.N., Thao, N.T.T., Nhi, P.T.T., Quan, N.T., Hoan, N.X., Nguyen, V.T. 2019. Impact of climate change on meteorological, hydrological and agricultural droughts in the Lower Mekong River Basin: A case study of the Srepok Basin, Vietnam. Water Environ. J. 33: 547-559.

Son, N.T., Chen, C., Chen, C., Chang, L., Minh, V.Q. 2012. Monitoring agricultural drought in the Lower Mekong Basin using MODIS NDVI and land surface temperature data. Int. J. Appl. Earth Obs. Geoinf. 18: 417-427.

Thao, N.T.T., Khoi, D.N., Denis, A., Viet, L.V., Wellens, J., Tychon, B. 2022. Early prediction of coffee yield in the Central Highlands of Vietnam using a statistical approach and satellite remote sensing vegetation biophysical variables. Remote Sens. 14: 2975.

Tiemann, T., Aye, T.M., Dung, N.D., Tien, T.M., Fisher, M., de Paulo, E.N., Oberthür, T. 2018. Crop nutrition for Vietnamese robusta coffee. Better Crops with Plant Food 102 : 20−23.

Tram, V.N.Q., Somura, H., Moroizumi, T. 2021. Evaluation of drought features in the Dakbla watershed, Central Highlands of Vietnam. Hydrological Research Letters 15: 77-83.

Tran, H.T., Campbell, J.B., Tran, T.D., Tran, H.T. 2017. Monitoring drought vulnerability using multispectral indices observed from sequential remote sensing (Case Study: Tuy Phong, Binh Thuan, Vietnam). GISci. Remote Sens. 54: 167−184.

Usman, U., Yelwa, S., Gulumbe, S., Danbaba, A., Nir, R. 2013. Modelling relationship between NDVI and climatic variables using geographically weighted regression. J. Math. Sci. Appl. 1: 24−28.

Van Viet, L. 2021. Development of a new ENSO index to assess the effects of ENSO on temperature over southern Vietnam. Theor. Appl. Climatol. 144: 1119−1129.

Van Viet, L., Thuy, T.T.T. 2023. Improving the quality of coffee yield forecasting in Dak Lak Province, Vietnam, through the utilization of remote sensing data. Environ. Res. Commun. 5: 095011.

Vélez-Nicolás, M., García-López, S., Ruiz-Ortiz, V., Zazo, S., and Molina, J.L. 2022. Precipitation variability and drought assessment using the SPI: Application to long-term series in the Strait of Gibraltar area. Water 14: 884.

Venancio, L.P., Filgueiras, R., Mantovani, E.C., et al. 2020. Impact of drought associated with high temperatures on *Coffea canephora* plantations: A case study in Espírito Santo State, Brazil. Sci. Rep. 10: 19719.

Vicente-Serrano, S.M., Beguería, S., López-Moreno, J.I. 2010. A multiscalar drought index sensitive to global warming: the standardized precipitation evapotranspiration index. J. Clim. 23: 1696−1718.

Vicente-Serrano, S.M., Quiring, S.M., Pena-Gallardo, M., Yuan, S., Dominguez-Castro, F. 2020. A review of environmental droughts: Increased risk under global warming? Earth Sci. Rev. 201: 102953.

Zargar, A., Sadiq, R., Naser, B., Khan, F.I. 2011. A review of drought indices. Environ. Rev. 19: 333−349.